#Exploration: A Study of Count-Based Exploration for Deep Reinforcement Learning

Haoran Tang[1][*], **Rein Houthooft**[34][*] , **Davis Foote**[2], **Adam Stooke**[2], **Xi Chen**[2][†],
Yan Duan[2][†], **John Schulman**[4], **Filip De Turck**[3], **Pieter Abbeel** [2][†]

[1] UC Berkeley, Department of Mathematics
[2] UC Berkeley, Department of Electrical Engineering and Computer Sciences
[3] Ghent University – imec, Department of Information Technology
[4] OpenAI

Abstract

Count-based exploration algorithms are known to perform near-optimally when used in conjunction with tabular reinforcement learning (RL) methods for solving small discrete Markov decision processes (MDPs). It is generally thought that count-based methods cannot be applied in high-dimensional state spaces, since most states will only occur once. Recent deep RL exploration strategies are able to deal with high-dimensional continuous state spaces through complex heuristics, often relying on *optimism in the face of uncertainty* or *intrinsic motivation*. In this work, we describe a surprising finding: a simple generalization of the classic count-based approach can reach near state-of-the-art performance on various high-dimensional and/or continuous deep RL benchmarks. States are mapped to hash codes, which allows to count their occurrences with a hash table. These counts are then used to compute a reward bonus according to the classic count-based exploration theory. We find that simple hash functions can achieve surprisingly good results on many challenging tasks. Furthermore, we show that a domain-dependent learned hash code may further improve these results. Detailed analysis reveals important aspects of a good hash function: 1) having appropriate granularity and 2) encoding information relevant to solving the MDP. This exploration strategy achieves near state-of-the-art performance on both continuous control tasks and Atari 2600 games, hence providing a simple yet powerful baseline for solving MDPs that require considerable exploration.

1 Introduction

Reinforcement learning (RL) studies an agent acting in an initially unknown environment, learning through trial and error to maximize rewards. It is impossible for the agent to act near-optimally until it has sufficiently explored the environment and identified all of the opportunities for high reward, in all scenarios. A core challenge in RL is how to balance exploration—actively seeking out novel states and actions that might yield high rewards and lead to long-term gains; and exploitation—maximizing short-term rewards using the agent's current knowledge. While there are exploration techniques for finite MDPs that enjoy theoretical guarantees, there are no fully satisfying techniques for high-dimensional state spaces; therefore, developing more general and robust exploration techniques is an active area of research.

---

[*]These authors contributed equally. Correspondence to: Haoran Tang <hrtang@math.berkeley.edu>, Rein Houthooft <rein.houthooft@openai.com>

[†]Work done at OpenAI

Most of the recent state-of-the-art RL results have been obtained using simple exploration strategies such as uniform sampling [21] and i.i.d./correlated Gaussian noise [19, 30]. Although these heuristics are sufficient in tasks with well-shaped rewards, the sample complexity can grow exponentially (with state space size) in tasks with sparse rewards [25]. Recently developed exploration strategies for deep RL have led to significantly improved performance on environments with sparse rewards. Bootstrapped DQN [24] led to faster learning in a range of Atari 2600 games by training an ensemble of Q-functions. Intrinsic motivation methods using pseudo-counts achieve state-of-the-art performance on Montezuma's Revenge, an extremely challenging Atari 2600 game [4]. Variational Information Maximizing Exploration (VIME, [13]) encourages the agent to explore by acquiring information about environment dynamics, and performs well on various robotic locomotion problems with sparse rewards. However, we have not seen a very simple and fast method that can work across different domains.

Some of the classic, theoretically-justified exploration methods are based on counting state-action visitations, and turning this count into a bonus reward. In the bandit setting, the well-known UCB algorithm of [18] chooses the action a_t at time t that maximizes $\hat{r}(a_t) + \sqrt{\frac{2 \log t}{n(a_t)}}$ where $\hat{r}(a_t)$ is the estimated reward, and $n(a_t)$ is the number of times action a_t was previously chosen. In the MDP setting, some of the algorithms have similar structure, for example, Model Based Interval Estimation–Exploration Bonus (MBIE-EB) of [34] counts state-action pairs with a table $n(s, a)$ and adding a bonus reward of the form $\frac{\beta}{\sqrt{n(s,a)}}$ to encourage exploring less visited pairs. [16] show that the inverse-square-root dependence is optimal. MBIE and related algorithms assume that the augmented MDP is solved analytically at each timestep, which is only practical for small finite state spaces.

This paper presents a simple approach for exploration, which extends classic counting-based methods to high-dimensional, continuous state spaces. We discretize the state space with a hash function and apply a bonus based on the state-visitation count. The hash function can be chosen to appropriately balance generalization across states, and distinguishing between states. We select problems from rllab [8] and Atari 2600 [3] featuring sparse rewards, and demonstrate near state-of-the-art performance on several games known to be hard for naïve exploration strategies. The main strength of the presented approach is that it is fast, flexible and complementary to most existing RL algorithms.

In summary, this paper proposes a generalization of classic count-based exploration to high-dimensional spaces through hashing (Section 2); demonstrates its effectiveness on challenging deep RL benchmark problems and analyzes key components of well-designed hash functions (Section 4).

2 Methodology

2.1 Notation

This paper assumes a finite-horizon discounted Markov decision process (MDP), defined by $(\mathcal{S}, \mathcal{A}, \mathcal{P}, r, \rho_0, \gamma, T)$, in which $\mathcal{S}$ is the state space, $\mathcal{A}$ the action space, $\mathcal{P}$ a transition probability distribution, $r : \mathcal{S} \times \mathcal{A} \to \mathbb{R}$ a reward function, ρ_0 an initial state distribution, $\gamma \in (0, 1]$ a discount factor, and T the horizon. The goal of RL is to maximize the total expected discounted reward $\mathbb{E}_{\pi, \mathcal{P}} \left[\sum_{t=0}^{T} \gamma^t r(s_t, a_t) \right]$ over a policy π, which outputs a distribution over actions given a state.

2.2 Count-Based Exploration via Static Hashing

Our approach discretizes the state space with a hash function $\phi : \mathcal{S} \to \mathbb{Z}$. An exploration bonus $r^+ : \mathcal{S} \to \mathbb{R}$ is added to the reward function, defined as

$$r^+(s) = \frac{\beta}{\sqrt{n(\phi(s))}}, \tag{1}$$

where $\beta \in \mathbb{R}_{\geq 0}$ is the bonus coefficient. Initially the counts $n(\cdot)$ are set to zero for the whole range of ϕ. For every state s_t encountered at time step t, $n(\phi(s_t))$ is increased by one. The agent is trained with rewards $(r + r^+)$, while performance is evaluated as the sum of rewards without bonuses.

Algorithm 1: Count-based exploration through static hashing, using SimHash

---

1   Define state preprocessor $g : \mathcal{S} \to \mathbb{R}^D$

2   (In case of SimHash) Initialize $A \in \mathbb{R}^{k \times D}$ with entries drawn i.i.d. from the standard Gaussian distribution $\mathcal{N}(0, 1)$

3   Initialize a hash table with values $n(\cdot) \equiv 0$

4   **for** each iteration j **do**

5   Collect a set of state-action samples $\{(s_m, a_m)\}_{m=0}^{M}$ with policy π

6   Compute hash codes through any LSH method, e.g., for SimHash, $\phi(s_m) = \operatorname{sgn}(Ag(s_m))$

7   Update the hash table counts $\forall m : 0 \leq m \leq M$ as $n(\phi(s_m)) \leftarrow n(\phi(s_m)) + 1$

8   Update the policy π using rewards $\left\{ r(s_m, a_m) + \dfrac{\beta}{\sqrt{n(\phi(s_m))}} \right\}_{m=0}^{M}$ with any RL algorithm

---

Note that our approach is a departure from count-based exploration methods such as MBIE-EB since we use a state-space count $n(s)$ rather than a state-action count $n(s, a)$. State-action counts $n(s, a)$ are investigated in the Supplementary Material, but no significant performance gains over state counting could be witnessed. A possible reason is that the policy itself is sufficiently random to try most actions at a novel state.

Clearly the performance of this method will strongly depend on the choice of hash function ϕ. One important choice we can make regards the *granularity* of the discretization: we would like for "distant" states to be be counted separately while "similar" states are merged. If desired, we can incorporate prior knowledge into the choice of ϕ, if there would be a set of salient state features which are known to be relevant. A short discussion on this matter is given in the Supplementary Material.

Algorithm 1 summarizes our method. The main idea is to use locality-sensitive hashing (LSH) to convert continuous, high-dimensional data to discrete hash codes. LSH is a popular class of hash functions for querying nearest neighbors based on certain similarity metrics [2]. A computationally efficient type of LSH is SimHash [6], which measures similarity by angular distance. SimHash retrieves a binary code of state $s \in \mathcal{S}$ as

$$\phi(s) = \operatorname{sgn}(Ag(s)) \in \{-1, 1\}^k, \tag{2}$$

where $g : \mathcal{S} \to \mathbb{R}^D$ is an optional preprocessing function and A is a $k \times D$ matrix with i.i.d. entries drawn from a standard Gaussian distribution $\mathcal{N}(0, 1)$. The value for k controls the granularity: higher values lead to fewer collisions and are thus more likely to distinguish states.

2.3   Count-Based Exploration via Learned Hashing

When the MDP states have a complex structure, as is the case with image observations, measuring their similarity directly in pixel space fails to provide the semantic similarity measure one would desire. Previous work in computer vision [7, 20, 36] introduce manually designed feature representations of images that are suitable for semantic tasks including detection and classification. More recent methods learn complex features directly from data by training convolutional neural networks [12, 17, 31]. Considering these results, it may be difficult for a method such as SimHash to cluster states appropriately using only raw pixels.

Therefore, rather than using SimHash, we propose to use an autoencoder (AE) to learn meaningful hash codes in one of its hidden layers as a more advanced LSH method. This AE takes as input states s and contains one special dense layer comprised of D sigmoid functions. By rounding the sigmoid activations $b(s)$ of this layer to their closest binary number $\lfloor b(s) \rceil \in \{0, 1\}^D$, any state s can be binarized. This is illustrated in Figure 1 for a convolutional AE.

A problem with this architecture is that dissimilar inputs s_i, s_j can map to identical hash codes $\lfloor b(s_i) \rceil = \lfloor b(s_j) \rceil$, but the AE still reconstructs them perfectly. For example, if $b(s_i)$ and $b(s_j)$ have values 0.6 and 0.7 at a particular dimension, the difference can be exploited by deconvolutional layers in order to reconstruct s_i and s_j perfectly, although that dimension rounds to the same binary value. One can imagine replacing the bottleneck layer $b(s)$ with the hash codes $\lfloor b(s) \rceil$, but then gradients cannot be back-propagated through the rounding function. A solution is proposed by Gregor et al. [10] and Salakhutdinov & Hinton [28] is to inject uniform noise $U(-a, a)$ into the sigmoid
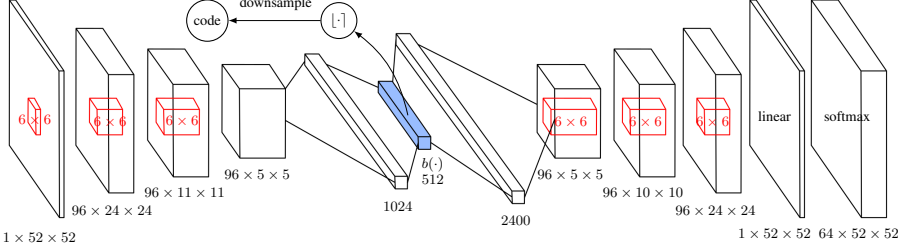
Figure 1: The autoencoder (AE) architecture for ALE; the solid block represents the dense sigmoidal binary code layer, after which noise $U(-a, a)$ is injected.

Algorithm 2: Count-based exploration using learned hash codes

---

1 Define state preprocessor $g : \mathcal{S} \to \{0, 1\}^D$ as the binary code resulting from the autoencoder (AE)
2 Initialize $A \in \mathbb{R}^{k \times D}$ with entries drawn i.i.d. from the standard Gaussian distribution $\mathcal{N}(0, 1)$
3 Initialize a hash table with values $n(\cdot) \equiv 0$
4 **for** each iteration j **do**
5   Collect a set of state-action samples $\{(s_m, a_m)\}_{m=0}^{M}$ with policy π
6   Add the state samples $\{s_m\}_{m=0}^{M}$ to a FIFO replay pool $\mathcal{R}$
7   **if** $j \bmod j_{\text{update}} = 0$ **then**
8   Update the AE loss function in Eq. (3) using samples drawn from the replay pool $\{s_n\}_{n=1}^{N} \sim \mathcal{R}$, for example using stochastic gradient descent
9   Compute $g(s_m) = \lfloor b(s_m) \rceil$, the D-dim rounded hash code for s_m learned by the AE
10   Project $g(s_m)$ to a lower dimension k via SimHash as $\phi(s_m) = \text{sgn}(A g(s_m))$
11   Update the hash table counts $\forall m : 0 \leq m \leq M$ as $n(\phi(s_m)) \leftarrow n(\phi(s_m)) + 1$
12   Update the policy π using rewards $\left\{ r(s_m, a_m) + \dfrac{\beta}{\sqrt{n(\phi(s_m))}} \right\}_{m=0}^{M}$ with any RL algorithm

---

activations. By choosing uniform noise with $a > \frac{1}{4}$, the AE is only capable of (always) reconstructing distinct state inputs $s_i \neq s_j$, if it has learned to spread the sigmoid outputs sufficiently far apart, $|b(s_i) - b(s_j)| > \epsilon$, in order to counteract the injected noise.

As such, the loss function over a set of collected states $\{s_i\}_{i=1}^{N}$ is defined as

$$L\left(\{s_n\}_{n=1}^{N}\right) = -\frac{1}{N} \sum_{n=1}^{N} \left[\log p(s_n) - \frac{\lambda}{K} \sum_{i=1}^{D} \min\left\{ (1 - b_i(s_n))^2, b_i(s_n)^2 \right\} \right], \quad (3)$$

with $p(s_n)$ the AE output. This objective function consists of a negative log-likelihood term and a term that pressures the binary code layer to take on binary values, scaled by $\lambda \in \mathbb{R}_{\geq 0}$. The reasoning behind this latter term is that it might happen that for particular states, a certain sigmoid unit is never used. Therefore, its value might fluctuate around $\frac{1}{2}$, causing the corresponding bit in binary code $\lfloor b(s) \rceil$ to flip over the agent lifetime. Adding this second loss term ensures that an unused bit takes on an arbitrary binary value.

For Atari 2600 image inputs, since the pixel intensities are discrete values in the range $[0, 255]$, we make use of a pixel-wise softmax output layer [37] that shares weights between all pixels. The architectural details are described in the Supplementary Material and are depicted in Figure 1. Because the code dimension often needs to be large in order to correctly reconstruct the input, we apply a downsampling procedure to the resulting binary code $\lfloor b(s) \rceil$, which can be done through random projection to a lower-dimensional space via SimHash as in Eq. (2).

On the one hand, it is important that the mapping from state to code needs to remain relatively consistent over time, which is nontrivial as the AE is constantly updated according to the latest data (Algorithm 2 line 8). A solution is to downsample the binary code to a very low dimension, or by slowing down the training process. On the other hand, the code has to remain relatively unique

for states that are both distinct and close together on the image manifold. This is tackled both by the second term in Eq. (3) and by the saturating behavior of the sigmoid units. States already well represented by the AE tend to saturate the sigmoid activations, causing the resulting loss gradients to be close to zero, making the code less prone to change.

3   Related Work

Classic count-based methods such as MBIE [33], MBIE-EB and [16] solve an approximate Bellman equation as an inner loop before the agent takes an action [34]. As such, bonus rewards are propagated immediately throughout the state-action space. In contrast, contemporary deep RL algorithms propagate the bonus signal based on rollouts collected from interacting with environments, with value-based [21] or policy gradient-based [22, 30] methods, at limited speed. In addition, our proposed method is intended to work with contemporary deep RL algorithms, it differs from classical count-based method in that our method relies on visiting unseen states first, before the bonus reward can be assigned, making uninformed exploration strategies still a necessity at the beginning. Filling the gaps between our method and classic theories is an important direction of future research.

A related line of classical exploration methods is based on the idea of *optimism in the face of uncertainty* [5] but not restricted to using counting to implement "optimism", e.g., R-Max [5], UCRL [14], and E^3 [15]. These methods, similar to MBIE and MBIE-EB, have theoretical guarantees in tabular settings.

Bayesian RL methods [9, 11, 16, 35], which keep track of a distribution over MDPs, are an alternative to optimism-based methods. Extensions to continuous state space have been proposed by [27] and [25].

Another type of exploration is curiosity-based exploration. These methods try to capture the agent's surprise about transition dynamics. As the agent tries to optimize for surprise, it naturally discovers novel states. We refer the reader to [29] and [26] for an extensive review on curiosity and intrinsic rewards.

Several exploration strategies for deep RL have been proposed to handle high-dimensional state space recently. [13] propose VIME, in which information gain is measured in Bayesian neural networks modeling the MDP dynamics, which is used an exploration bonus. [32] propose to use the prediction error of a learned dynamics model as an exploration bonus. Thompson sampling through bootstrapping is proposed by [24], using bootstrapped Q-functions.

The most related exploration strategy is proposed by [4], in which an exploration bonus is added inversely proportional to the square root of a *pseudo-count* quantity. A state pseudo-count is derived from its log-probability improvement according to a density model over the state space, which in the limit converges to the empirical count. Our method is similar to pseudo-count approach in the sense that both methods are performing approximate counting to have the necessary generalization over unseen states. The difference is that a density model has to be designed and learned to achieve good generalization for pseudo-count whereas in our case generalization is obtained by a wide range of simple hash functions (not necessarily SimHash). Another interesting connection is that our method also implies a density model $\rho(s) = \frac{n(\phi(s))}{N}$ over all visited states, where N is the total number of states visited. Another method similar to hashing is proposed by [1], which clusters states and counts cluster centers instead of the true states, but this method has yet to be tested on standard exploration benchmark problems.

4   Experiments

Experiments were designed to investigate and answer the following research questions:

1. Can count-based exploration through hashing improve performance significantly across different domains? How does the proposed method compare to the current state of the art in exploration for deep RL?

2. What is the impact of learned or static state preprocessing on the overall performance when image observations are used?

To answer question 1, we run the proposed method on deep RL benchmarks (rllab and ALE) that feature sparse rewards, and compare it to other state-of-the-art algorithms. Question 2 is answered by trying out different image preprocessors on Atari 2600 games. Trust Region Policy Optimization (TRPO, [30]) is chosen as the RL algorithm for all experiments, because it can handle both discrete and continuous action spaces, can conveniently ensure stable improvement in the policy performance, and is relatively insensitive to hyperparameter changes. The hyperparameters settings are reported in the Supplementary Material.

4.1 Continuous Control

The rllab benchmark [8] consists of various control tasks to test deep RL algorithms. We selected several variants of the basic and locomotion tasks that use sparse rewards, as shown in Figure 2, and adopt the experimental setup as defined in [13]—a description can be found in the Supplementary Material. These tasks are all highly difficult to solve with naïve exploration strategies, such as adding Gaussian noise to the actions.
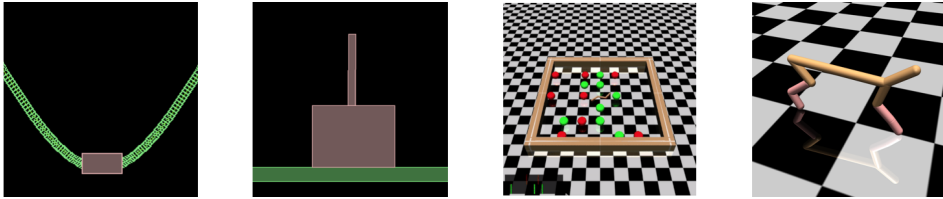

Figure 2: Illustrations of the rllab tasks used in the continuous control experiments, namely MountainCar, CartPoleSwingup, SimmerGather, and HalfCheetah; taken from [8].

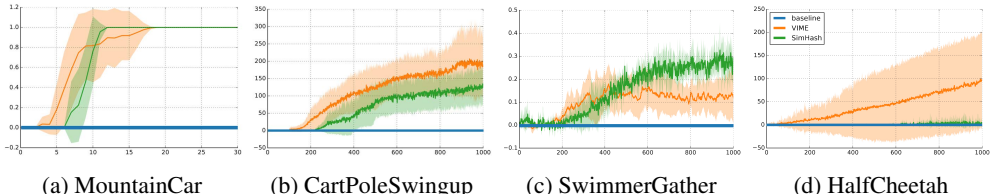| (a) MountainCar | (b) CartPoleSwingup | (c) SwimmerGather | (d) HalfCheetah |

Figure 3: Mean average return of different algorithms on rllab tasks with sparse rewards. The solid line represents the mean average return, while the shaded area represents one standard deviation, over 5 seeds for the baseline and SimHash (the baseline curves happen to overlap with the axis).

Figure 3 shows the results of TRPO (baseline), TRPO-SimHash, and VIME [13] on the classic tasks MountainCar and CartPoleSwingup, the locomotion task HalfCheetah, and the hierarchical task SwimmerGather. Using count-based exploration with hashing is capable of reaching the goal in all environments (which corresponds to a nonzero return), while baseline TRPO with Gaussia n control noise fails completely. Although TRPO-SimHash picks up the sparse reward on HalfCheetah, it does not perform as well as VIME. In contrast, the performance of SimHash is comparable with VIME on MountainCar, while it outperforms VIME on SwimmerGather.

4.2 Arcade Learning Environment

The Arcade Learning Environment (ALE, [3]), which consists of Atari 2600 video games, is an important benchmark for deep RL due to its high-dimensional state space and wide variety of games. In order to demonstrate the effectiveness of the proposed exploration strategy, six games are selected featuring long horizons while requiring significant exploration: Freeway, Frostbite, Gravitar, Montezuma's Revenge, Solaris, and Venture. The agent is trained for 500 iterations in all experiments, with each iteration consisting of $0.1\,\mathrm{M}$ steps (the TRPO batch size, corresponds to $0.4\,\mathrm{M}$ frames). Policies and value functions are neural networks with identical architectures to [22]. Although the policy and baseline take into account the previous four frames, the counting algorithm only looks at the latest frame.

Table 1: Atari 2600: average total reward after training for $50\,\mathrm{M}$ time steps. Boldface numbers indicate best results. Italic numbers are the best among our methods.

	Freeway	Frostbite	Gravitar	Montezuma	Solaris	Venture
TRPO (baseline)	16.5	2869	486	0	2758	121
TRPO-pixel-SimHash	31.6	4683	468	0	2897	263
TRPO-BASS-SimHash	28.4	3150	*604*	*238*	1201	*616*
TRPO-AE-SimHash	***33.5***	***5214***	482	75	*4467*	445
Double-DQN	33.3	1683	412	0	3068	98.0
Dueling network	0.0	4672	588	0	2251	497
Gorila	11.7	605	**1054**	4	N/A	**1245**
DQN Pop-Art	33.4	3469	483	0	**4544**	1172
A3C+	27.3	507	246	142	2175	0
pseudo-count	29.2	1450	–	**3439**	–	369

BASS To compare with the autoencoder-based learned hash code, we propose using Basic Abstraction of the ScreenShots (BASS, also called Basic; see [3]) as a static preprocessing function g. BASS is a hand-designed feature transformation for images in Atari 2600 games. BASS builds on the following observations specific to Atari: 1) the game screen has a low resolution, 2) most objects are large and monochrome, and 3) winning depends mostly on knowing object locations and motions. We designed an adapted version of BASS[3], that divides the RGB screen into square cells, computes the average intensity of each color channel inside a cell, and assigns the resulting values to bins that uniformly partition the intensity range $[0, 255]$. Mathematically, let C be the cell size (width and height), B the number of bins, (i, j) cell location, (x, y) pixel location, and z the channel, then

$$\text{feature}(i, j, z) = \left\lfloor \frac{B}{255C^2} \sum_{(x,y) \in \text{cell}(i,j)} I(x, y, z) \right\rfloor. \tag{4}$$

Afterwards, the resulting integer-valued feature tensor is converted to an integer hash code ($\phi(s_t)$ in Line 6 of Algorithm 1). A BASS feature can be regarded as a miniature that efficiently encodes object locations, but remains invariant to negligible object motions. It is easy to implement and introduces little computation overhead. However, it is designed for generic Atari game images and may not capture the structure of each specific game very well.

We compare our results to double DQN [39], dueling network [40], A3C+ [4], double DQN with pseudo-counts [4], Gorila [23], and DQN Pop-Art [38] on the "null op" metric[4]. We show training curves in Figure 4 and summarize all results in Table 1. Surprisingly, TRPO-pixel-SimHash already outperforms the baseline by a large margin and beats the previous best result on Frostbite. TRPO-BASS-SimHash achieves significant improvement over TRPO-pixel-SimHash on Montezuma's Revenge and Venture, where it captures object locations better than other methods.[5] TRPO-AE-SimHash achieves near state-of-the-art performance on Freeway, Frostbite and Solaris.

As observed in Table 1, preprocessing images with BASS or using a learned hash code through the AE leads to much better performance on Gravitar, Montezuma's Revenge and Venture. Therefore, a static or adaptive preprocessing step can be important for a good hash function.

In conclusion, our count-based exploration method is able to achieve remarkable performance gains even with simple hash functions like SimHash on the raw pixel space. If coupled with domain-dependent state preprocessing techniques, it can sometimes achieve far better results.

A reason why our proposed method does not achieve state-of-the-art performance on all games is that TRPO does not reuse off-policy experience, in contrast to DQN-based algorithms [4, 23, 38]), and is

---

[3]The original BASS exploits the fact that at most 128 colors can appear on the screen. Our adapted version does not make this assumption.

[4]The agent takes no action for a random number (within 30) of frames at the beginning of each episode.

[5]We provide videos of example game play and visualizations of the difference bewteen Pixel-SimHash and BASS-SimHash at https://www.youtube.com/playlist?list=PLAd-UMX6FkBQdLNWtY8nH1-pzYJA_1T55

(a) Freeway   (b) Frostbite   (c) Gravitar

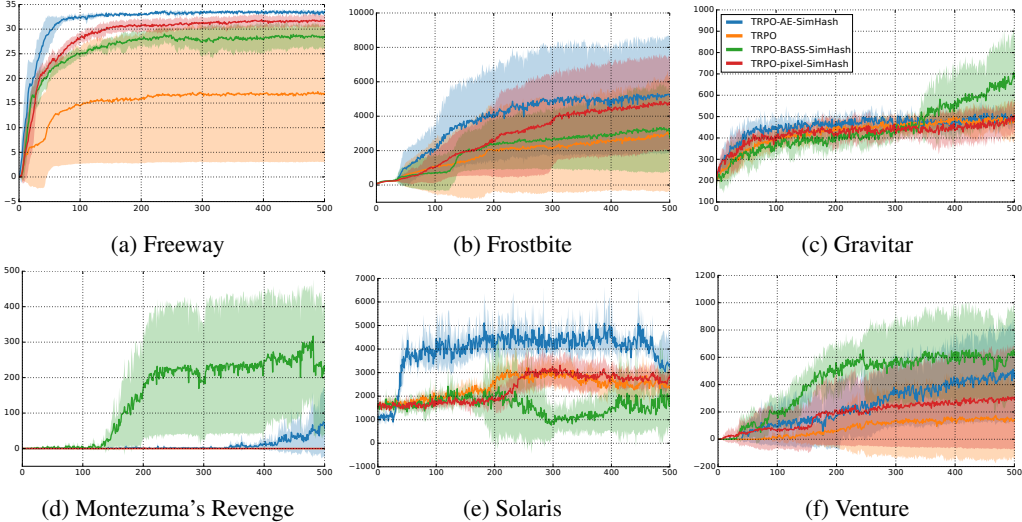(d) Montezuma's Revenge   (e) Solaris   (f) Venture

Figure 4: Atari 2600 games: the solid line is the mean average undiscounted return per iteration, while the shaded areas represent the one standard deviation, over 5 seeds for the baseline, TRPO-pixel-SimHash, and TRPO-BASS-SimHash, while over 3 seeds for TRPO-AE-SimHash.

hence less efficient in harnessing extremely sparse rewards. This explanation is corroborated by the experiments done in [4], in which A3C+ (an on-policy algorithm) scores much lower than DQN (an off-policy algorithm), while using the exact same exploration bonus.

5   Conclusions

This paper demonstrates that a generalization of classical counting techniques through hashing is able to provide an appropriate signal for exploration, even in continuous and/or high-dimensional MDPs using function approximators, resulting in near state-of-the-art performance across benchmarks. It provides a simple yet powerful baseline for solving MDPs that require informed exploration.

Acknowledgments

References

[1] Abel, David, Agarwal, Alekh, Diaz, Fernando, Krishnamurthy, Akshay, and Schapire, Robert E. Exploratory gradient boosting for reinforcement learning in complex domains. *arXiv preprint arXiv:1603.04119*, 2016.

[2] Andoni, Alexandr and Indyk, Piotr. Near-optimal hashing algorithms for approximate nearest neighbor in high dimensions. In *Proceedings of the 47th Annual IEEE Symposium on Foundations of Computer Science (FOCS)*, pp. 459–468, 2006.

[3] Bellemare, Marc G, Naddaf, Yavar, Veness, Joel, and Bowling, Michael. The arcade learning environment: An evaluation platform for general agents. *Journal of Artificial Intelligence Research*, 47:253–279, 06 2013.

[4] Bellemare, Marc G, Srinivasan, Sriram, Ostrovski, Georg, Schaul, Tom, Saxton, David, and Munos, Remi. Unifying count-based exploration and intrinsic motivation. In *Advances in Neural Information Processing Systems 29 (NIPS)*, pp. 1471–1479, 2016.

[5] Brafman, Ronen I and Tennenholtz, Moshe. R-max-a general polynomial time algorithm for near-optimal reinforcement learning. *Journal of Machine Learning Research*, 3:213–231, 2002.

[6] Charikar, Moses S. Similarity estimation techniques from rounding algorithms. In *Proceedings of the 34th Annual ACM Symposium on Theory of Computing (STOC)*, pp. 380–388, 2002.

[7] Dalal, Navneet and Triggs, Bill. Histograms of oriented gradients for human detection. In *Proceedings of the IEEE International Conference on Computer Vision and Pattern Recognition (CVPR)*, pp. 886–893, 2005.

[8] Duan, Yan, Chen, Xi, Houthooft, Rein, Schulman, John, and Abbeel, Pieter. Benchmarking deep reinforcement learning for continous control. In *Proceedings of the 33rd International Conference on Machine Learning (ICML)*, pp. 1329–1338, 2016.

[9] Ghavamzadeh, Mohammad, Mannor, Shie, Pineau, Joelle, and Tamar, Aviv. Bayesian reinforcement learning: A survey. *Foundations and Trends in Machine Learning*, 8(5-6):359–483, 2015.

[10] Gregor, Karol, Besse, Frederic, Jimenez Rezende, Danilo, Danihelka, Ivo, and Wierstra, Daan. Towards conceptual compression. In *Advances in Neural Information Processing Systems 29 (NIPS)*, pp. 3549–3557. 2016.

[11] Guez, Arthur, Heess, Nicolas, Silver, David, and Dayan, Peter. Bayes-adaptive simulation-based search with value function approximation. In *Advances in Neural Information Processing Systems (Advances in Neural Information Processing Systems (NIPS))*, pp. 451–459, 2014.

[12] He, Kaiming, Zhang, Xiangyu, Ren, Shaoqing, and Sun, Jian. Deep residual learning for image recognition. 2015.

[13] Houthooft, Rein, Chen, Xi, Duan, Yan, Schulman, John, De Turck, Filip, and Abbeel, Pieter. VIME: Variational information maximizing exploration. In *Advances in Neural Information Processing Systems 29 (NIPS)*, pp. 1109–1117, 2016.

[14] Jaksch, Thomas, Ortner, Ronald, and Auer, Peter. Near-optimal regret bounds for reinforcement learning. *Journal of Machine Learning Research*, 11:1563–1600, 2010.

[15] Kearns, Michael and Singh, Satinder. Near-optimal reinforcement learning in polynomial time. *Machine Learning*, 49(2-3):209–232, 2002.

[16] Kolter, J Zico and Ng, Andrew Y. Near-bayesian exploration in polynomial time. In *Proceedings of the 26th International Conference on Machine Learning (ICML)*, pp. 513–520, 2009.

[17] Krizhevsky, Alex, Sutskever, Ilya, and Hinton, Geoffrey E. ImageNet classification with deep convolutional neural networks. In *Advances in Neural Information Processing Systems 25 (NIPS)*, pp. 1097–1105, 2012.

[18] Lai, Tze Leung and Robbins, Herbert. Asymptotically efficient adaptive allocation rules. *Advances in Applied Mathematics*, 6(1):4–22, 1985.

[19] Lillicrap, Timothy P, Hunt, Jonathan J, Pritzel, Alexander, Heess, Nicolas, Erez, Tom, Tassa, Yuval, Silver, David, and Wierstra, Daan. Continuous control with deep reinforcement learning. *arXiv preprint arXiv:1509.02971*, 2015.

[20] Lowe, David G. Object recognition from local scale-invariant features. In *Proceedings of the 7th IEEE International Conference on Computer Vision (ICCV)*, pp. 1150–1157, 1999.

[21] Mnih, Volodymyr, Kavukcuoglu, Koray, Silver, David, Rusu, Andrei A, Veness, Joel, Bellemare, Marc G, Graves, Alex, Riedmiller, Martin, Fidjeland, Andreas K, Ostrovski, Georg, et al. Human-level control through deep reinforcement learning. *Nature*, 518(7540):529–533, 2015.

[22] Mnih, Volodymyr, Badia, Adria Puigdomenech, Mirza, Mehdi, Graves, Alex, Lillicrap, Timothy P, Harley, Tim, Silver, David, and Kavukcuoglu, Koray. Asynchronous methods for deep reinforcement learning. *arXiv preprint arXiv:1602.01783*, 2016.

[23] Nair, Arun, Srinivasan, Praveen, Blackwell, Sam, Alcicek, Cagdas, Fearon, Rory, De Maria, Alessandro, Panneershelvam, Vedavyas, Suleyman, Mustafa, Beattie, Charles, Petersen, Stig, et al. Massively parallel methods for deep reinforcement learning. *arXiv preprint arXiv:1507.04296*, 2015.

[24] Osband, Ian, Blundell, Charles, Pritzel, Alexander, and Van Roy, Benjamin. Deep exploration via bootstrapped DQN. In *Advances in Neural Information Processing Systems 29 (NIPS)*, pp. 4026–4034, 2016.

[25] Osband, Ian, Van Roy, Benjamin, and Wen, Zheng. Generalization and exploration via randomized value functions. In *Proceedings of the 33rd International Conference on Machine Learning (ICML)*, pp. 2377–2386, 2016.

[26] Oudeyer, Pierre-Yves and Kaplan, Frederic. What is intrinsic motivation? A typology of computational approaches. *Frontiers in Neurorobotics*, 1:6, 2007.

[27] Pazis, Jason and Parr, Ronald. PAC optimal exploration in continuous space Markov decision processes. In *Proceedings of the 27th AAAI Conference on Artificial Intelligence (AAAI)*, 2013.

[28] Salakhutdinov, Ruslan and Hinton, Geoffrey. Semantic hashing. *International Journal of Approximate Reasoning*, 50(7):969 – 978, 2009.

[29] Schmidhuber, Jürgen. Formal theory of creativity, fun, and intrinsic motivation (1990–2010). *IEEE Transactions on Autonomous Mental Development*, 2(3):230–247, 2010.

[30] Schulman, John, Levine, Sergey, Moritz, Philipp, Jordan, Michael I, and Abbeel, Pieter. Trust region policy optimization. In *Proceedings of the 32nd International Conference on Machine Learning (ICML)*, 2015.

[31] Simonyan, Karen and Zisserman, Andrew. Very deep convolutional networks for large-scale image recognition. *arXiv preprint arXiv:1409.1556*, 2014.

[32] Stadie, Bradly C, Levine, Sergey, and Abbeel, Pieter. Incentivizing exploration in reinforcement learning with deep predictive models. *arXiv preprint arXiv:1507.00814*, 2015.

[33] Strehl, Alexander L and Littman, Michael L. A theoretical analysis of model-based interval estimation. In *Proceedings of the 21st International Conference on Machine Learning (ICML)*, pp. 856–863, 2005.

[34] Strehl, Alexander L and Littman, Michael L. An analysis of model-based interval estimation for Markov decision processes. *Journal of Computer and System Sciences*, 74(8):1309–1331, 2008.

[35] Sun, Yi, Gomez, Faustino, and Schmidhuber, Jürgen. Planning to be surprised: Optimal Bayesian exploration in dynamic environments. In *Proceedings of the 4th International Conference on Artificial General Intelligence (AGI)*, pp. 41–51. 2011.

[36] Tola, Engin, Lepetit, Vincent, and Fua, Pascal. DAISY: An efficient dense descriptor applied to wide-baseline stereo. *IEEE Transactions on Pattern Analysis and Machine Intelligence*, 32(5): 815–830, 2010.

[37] van den Oord, Aaron, Kalchbrenner, Nal, and Kavukcuoglu, Koray. Pixel recurrent neural networks. In *Proceedings of the 33rd International Conference on Machine Learning (ICML)*, pp. 1747–1756, 2016.

[38] van Hasselt, Hado, Guez, Arthur, Hessel, Matteo, and Silver, David. Learning functions across many orders of magnitudes. *arXiv preprint arXiv:1602.07714*, 2016.

[39] van Hasselt, Hado, Guez, Arthur, and Silver, David. Deep reinforcement learning with double Q-learning. In *Proceedings of the 30th AAAI Conference on Artificial Intelligence (AAAI)*, 2016.

[40] Wang, Ziyu, de Freitas, Nando, and Lanctot, Marc. Dueling network architectures for deep reinforcement learning. In *Proceedings of the 33rd International Conference on Machine Learning (ICML)*, pp. 1995–2003, 2016.

Supplementary Material

Anonymous Author(s)
Affiliation
Address
`email`

1 Hyperparameter Settings

Throughout all experiments, we use Adam [8] for optimizing the baseline function and the autoencoder. Hyperparameters for rllab experiments are summarized in Table 1. Here the policy takes a state s as input, and outputs a Gaussian distribution $\mathcal{N}(\mu(s), \sigma^2)$, where $\mu(s)$ is the output of a multi-layer perceptron (MLP) with `tanh` nonlinearity, and $\sigma > 0$ is a state-independent parameter.

Table 1: TRPO hyperparameters for rllab experiments

Experiment	MountainCar	CartPoleSwingUp	HalfCheetah	SwimmerGatherer
TRPO batch size	5k	5k	5k	50k
TRPO step size		0.01		
Discount factor γ		0.99		
Policy hidden units	(32, 32)	(32,)	(32, 32)	(64, 32)
Baseline function	linear	linear	linear	MLP: 32 units
Exploration bonus		$\beta = 0.01$		
SimHash dimension		$k = 32$		

Hyperparameters for Atari 2600 experiments are summarized in Table 2 and 3. By default, all convolutional layers are followed by ReLU nonlinearity.

Table 2: TRPO hyperparameters for Atari experiments with image input

Experiment	TRPO-pixel-SimHash	TRPO-BASS-SimHash	TRPO-AE-SimHash
TRPO batch size		100k	
TRPO step size		0.01	
Discount factor		0.995	
# random seeds	5	5	3
Input preprocessing	grayscale; downsampled to 52×52; each pixel rescaled to $[-1, 1]$		
	4 previous frames are concatenated to form the input state		
Policy structure	16 conv filters of size 8×8, stride 4		
	32 conv filters of size 4×4, stride 2		
	fully-connect layer with 256 units		
	linear transform and softmax to output action probabilities		
	(use batch normalization[7] at every layer)		
Baseline structure	(same as policy, except that the last layer is a single scalar)		
Exploration bonus		$\beta = 0.01$	
Hashing parameters	$k = 256$	cell size $C = 20$	$b(s)$ size: 256 bits
		$B = 20$ bins	downsampled to 64 bits

The autoencoder architecture was shown in Figure 1 of Section 2.3. Specifically, uniform noise $U(-a, a)$ with $a = 0.3$ is added to the sigmoid activations. The loss function Eq.(3) (in the main

Table 3: TRPO hyperparameters for Atari experiments with RAM input

Experiment	TRPO-RAM-SimHash
TRPO batch size	100k
TRPO step size	0.01
Discount factor	0.995
# random seeds	10
Input preprocessing	vector of length 128 in the range $[0, 255]$; downsampled to $[-1, 1]$
Policy structure	MLP: (32, 32, number_of_actions), $\tanh$
Baseline structure	MLP: (32, 32, 1), $\tanh$
Exploration bonus	$\beta = 0.01$
SimHash dimension	$k = 256$

text), using $\lambda = 10$, is updated every $j_{\text{update}} = 3$ iterations. The architecture looks as follows: an input layer of size 52×52, representing the image luminance is followed by 3 consecutive 6×6 convolutional layers with stride 2 and 96 filters feed into a fully connected layer of size 1024, which connects to the binary code layer. This binary code layer feeds into a fully-connected layer of 1024 units, connecting to a fully-connected layer of 2400 units. This layer feeds into 3 consecutive 6×6 transposed convolutional layers of which the final one connects to a pixel-wise softmax layer with 64 bins, representing the pixel intensities. Moreover, label smoothing is applied to the different softmax bins, in which the log-probability of each of the bins is increased by 0.003, before normalizing. The softmax weights are shared among each pixel.

In addition, we apply counting Bloom filters [5] to maintain a small hash table. Details can be found in Appendix 4.

2   Description of the Adapted rllab Tasks

This section describes the continuous control environments used in the experiments. The tasks are implemented as described in [4], following the sparse reward adaptation of [6]. The tasks have the following state and action dimensions: CartPoleSwingup, $\mathcal{S} \subseteq \mathbb{R}^4$, $\mathcal{A} \subseteq \mathbb{R}$; MountainCar $\mathcal{S} \subseteq \mathbb{R}^3$, $\mathcal{A} \subseteq \mathbb{R}^1$; HalfCheetah, $\mathcal{S} \subseteq \mathbb{R}^{20}$, $\mathcal{A} \subseteq \mathbb{R}^6$; SwimmerGather, $\mathcal{S} \subseteq \mathbb{R}^{33}$, $\mathcal{A} \subseteq \mathbb{R}^2$. For the sparse reward experiments, the tasks have been modified as follows. In CartPoleSwingup, the agent receives a reward of $+1$ when $\cos(\beta) > 0.8$, with β the pole angle. In MountainCar, the agent receives a reward of $+1$ when the goal state is reached, namely escaping the valley from the right side. Therefore, the agent has to figure out how to swing up the pole in the absence of any initial external rewards. In HalfCheetah, the agent receives a reward of $+1$ when $x_{\text{body}} > 5$. As such, it has to figure out how to move forward without any initial external reward. The time horizon is set to $T = 500$ for all tasks.

3   Analysis of Learned Binary Representation

Figure 1 shows the downsampled codes learned by the autoencoder for several Atari 2600 games (Frostbite, Freeway, and Montezuma's Revenge). Each row depicts 50 consecutive frames (from 0 to 49, going from left to right, top to bottom). The pictures in the right column depict the binary codes that correspond with each of these frames (one frame per row). Figure 2 shows the reconstructions of several subsequent images according to the autoencoder. Some binaries stay consistent across frames, and some appear to respond to specific objects or events. Although the precise meaning of each binary number is not immediately obvious, the figure suggests that the learned hash code is a reasonable abstraction of the game state.

4   Counting Bloom Filter/Count-Min Sketch

We experimented with directly building a hashing dictionary with keys $\phi(s)$ and values the state counts, but observed an unnecessary increase in computation time. Our implementation converts the integer hash codes into binary numbers and then into the "bytes" type in Python. The hash table is a dictionary using those bytes as keys.
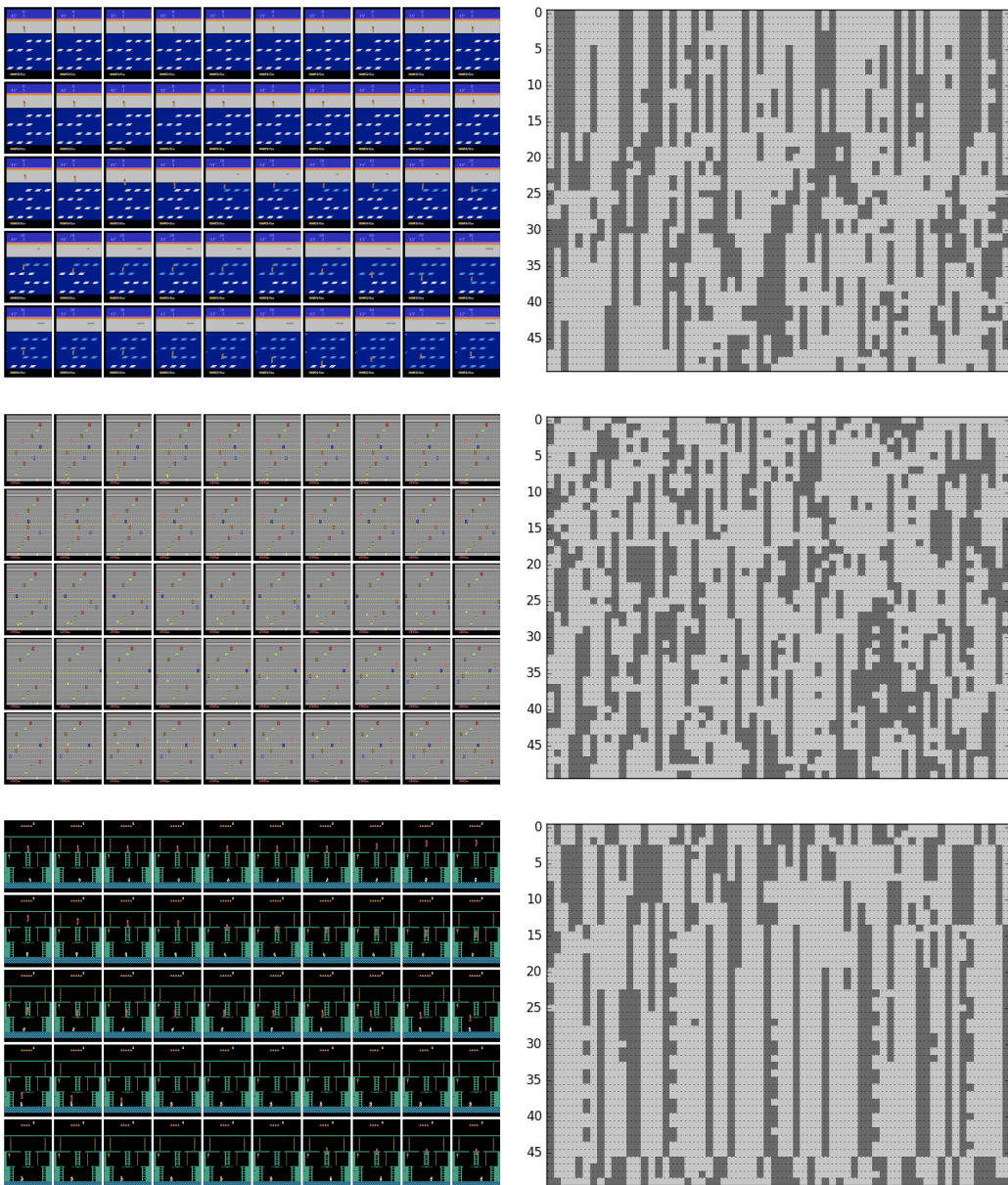
Figure 1: Frostbite, Freeway, and Montezuma's Revenge: subsequent frames (left) and corresponding code (right); the frames are ordered from left (starting with frame number 0) to right, top to bottom; the vertical axis in the right images correspond to the frame number.

However, an alternative technique called Count-Min Sketch [3], with a data structure identical to counting Bloom filters [5], can count with a fixed integer array and thus reduce computation time. Specifically, let $p^1, \ldots, p^l$ be distinct large prime numbers and define $\phi^j(s) = \phi(s) \mod p^j$. The count of state s is returned as $\min_{1 \leq j \leq l} n^j\big(\phi^j(s)\big)$. To increase the count of s, we increment $n^j\big(\phi^j(s)\big)$ by 1 for all j. Intuitively, the method replaces ϕ by weaker hash functions, while it reduces the probability of over-counting by reporting counts agreed by all such weaker hash functions. The final hash code is represented as $\big(\phi^1(s), \ldots, \phi^l(s)\big)$.

Throughout all experiments above, the prime numbers for the counting Bloom filter are 999931, 999953, 999959, 999961, 999979, and 999983, which we abbreviate as "6 M". In addition, we experimented with 6 other prime numbers, each approximately 15 M, which we abbreviate as "90 M". As we can see in Figure 3, counting states with a dictionary or with Bloom filters lead to similar performance, but the computation time of latter is lower. Moreover, there is little difference between direct counting and using a very larger table for Bloom filters, as the average bonus rewards are almost the same, indicating the same degree of exploration-exploitation trade-off. On the other hand, Bloom filters require a fixed table size, which may not be known beforehand.

Theory of Bloom Filters   Bloom filters [2] are popular for determining whether a data sample s' belongs to a dataset $\mathcal{D}$. Suppose we have l functions ϕ^j that independently assign each data sample to an integer between 1 and p uniformly at random. Initially $1, 2, \ldots, p$ are marked as 0. Then every $s \in \mathcal{D}$ is "inserted" through marking $\phi^j(s)$ as 1 for all j. A new sample s' is reported as a member of $\mathcal{D}$ only if $\phi^j(s)$ are marked as 1 for all j. A bloom filter has zero false negative rate (any $s \in \mathcal{D}$ is reported a member), while the false positive rate (probability of reporting a nonmember as a member) decays exponentially in l.

Though Bloom filters support data insertion, it does not allow data deletion. Counting Bloom filters [5] maintain a counter $n(\cdot)$ for each number between 1 and p. Inserting/deleting s corresponds to incrementing/decrementing $n\big(\phi^j(s)\big)$ by 1 for all j. Similarly, s is considered a member if $\forall j : n\big(\phi^j(s)\big) = 0$.

Count-Min sketch is designed to support memory-efficient counting without introducing too many over-counts. It maintains a separate count n^j for each hash function ϕ^j defined as $\phi^j(s) = \phi(s) \mod p^j$, where p^j is a large prime number. For simplicity, we may assume that $p^j \approx p \; \forall j$ and ϕ^j assigns s to any of $1, \ldots, p$ with uniform probability.

We now derive the probability of over-counting. Let s be a fixed data sample (not necessarily inserted yet) and suppose a dataset $\mathcal{D}$ of N samples are inserted. We assume that $p^l \gg N$. Let $n := \min_{1 \leq j \leq l} n^j\big(\phi^j(s)\big)$ be the count returned by the Bloom filter. We are interested in computing $\mathrm{Prob}(n > 0 | s \notin \mathcal{D})$. Due to assumptions about ϕ^j, we know $n^j(\phi(s)) \sim \mathrm{Binomial}\left(N, \frac{1}{p}\right)$. Therefore,

$$
\begin{aligned}
\mathrm{Prob}(n > 0 | s \notin \mathcal{D}) &= \frac{\mathrm{Prob}(n > 0, s \notin \mathcal{D})}{\mathrm{Prob}(s \notin \mathcal{D})} \\
&= \frac{\mathrm{Prob}(n > 0) - \mathrm{Prob}(s \in \mathcal{D})}{\mathrm{Prob}(s \notin \mathcal{D})} \\
&\approx \frac{\mathrm{Prob}(n > 0)}{\mathrm{Prob}(s \notin \mathcal{D})} \\
&= \frac{\prod_{j=1}^l \mathrm{Prob}(n^j(\phi^j(s)) > 0)}{(1 - 1/p^l)^N} \\
&= \frac{(1 - (1 - 1/p)^N)^l}{(1 - 1/p^l)^N} \\
&\approx \frac{(1 - e^{-N/p})^l}{e^{-N/p^l}} \\
&\approx (1 - e^{-N/p})^l.
\end{aligned}
\tag{1}
$$

In particular, the probability of over-counting decays exponentially in l. We refer the readers to [3] for other properties of the Count-Min sketch.

4

5   Robustness Analysis

5.1   Granularity

While our proposed method is able to achieve remarkable results without requiring much tuning, the granularity of the hash function should be chosen wisely. Granularity plays a critical role in count-based exploration, where the hash function should cluster states without under-generalizing or over-generalizing. Table 4 summarizes granularity parameters for our hash functions. In Table 5 we summarize the performance of TRPO-pixel-SimHash under different granularities. We choose Frostbite and Venture on which TRPO-pixel-SimHash outperforms the baseline, and choose as reward bonus coefficient $\beta = 0.01 \times \frac{256}{k}$ to keep average bonus rewards at approximately the same scale. $k = 16$ only corresponds to 65536 distinct hash codes, which is insufficient to distinguish between semantically distinct states and hence leads to worse performance. We observed that $k = 512$ tends to capture trivial image details in Frostbite, leading the agent to believe that every state is new and equally worth exploring. Similar results are observed while tuning the granularity parameters for TRPO-BASS-SimHash and TRPO-AE-SimHash.

Table 4: Granularity parameters of various hash functions

SimHash	k: size of the binary code
BASS	C: cell size
	B: number of bins for each color channel
AE	k: downstream SimHash parameter
	λ: binarization parameter
SmartHash	s: grid size agent (x, y) coordinates

Table 5: Average score at $50\,\mathrm{M}$ time steps achieved by TRPO-pixel-SimHash

k	16	64	128	256	512
Frostbite	3326	4029	3932	**4683**	1117
Venture	0	218	142	263	**306**

The best granularity depends on both the hash function and the MDP. While adjusting granularity parameter, we observed that it is important to lower the bonus coefficient as granularity is increased. This is because a higher granularity is likely to cause lower state counts, leading to higher bonus rewards that may overwhelm the true rewards.

Apart from the experimental results shown in Table 1 in the main text and Table 5, additional experiments have been performed to study several properties of our algorithm.

5.2   Hyperparameter sensitivity

To study the performance sensitivity to hyperparameter changes, we focus on evaluating TRPO-RAM-SimHash on the Atari 2600 game Frostbite, where the method has a clear advantage over the baseline. Because the final scores can vary between different random seeds, we evaluated each set of hyperparameters with 30 seeds. To reduce computation time and cost, RAM states are used instead of image observations.

The results are summarized in Table 6. Herein, k refers to the length of the binary code for hashing while β is the multiplicative coefficient for the reward bonus, as defined in Section 2.2 of the main text. This table demonstrates that most hyperparameter settings outperform the baseline ($\beta = 0$) significantly. Moreover, the final scores show a clear pattern in response to changing hyperparameters. Small β-values lead to insufficient exploration, while large β-values cause the bonus rewards to overwhelm the true rewards. With a fixed k, the scores are roughly concave in β, peaking at around 0.2. Higher granularity k leads to better performance. Therefore, it can be concluded that the proposed exploration method is robust to hyperparameter changes in comparison to the baseline, and that the best parameter settings can be obtained from a relatively coarse-grained grid search.

5

Table 6: TRPO-RAM-SimHash performance robustness to hyperparameter changes on Frostbite

k	β							
	0	0.01	0.05	0.1	0.2	0.4	0.8	1.6
–	397	–	–	–	–	–	–	–
64	–	879	2464	2243	2489	1587	1107	441
128	–	1475	4248	2801	3239	3621	1543	395
256	–	2583	4497	4437	7849	3516	2260	374

Table 7: Average score at $50\,\mathrm{M}$ time steps achieved by TRPO-SmartHash on Montezuma's Revenge (RAM observations)

s	1	5	10	20	40	60
score	2598	2500	**3533**	3025	2500	1921

Table 8: Interpretation of particular RAM entries in Montezuma's Revenge

ID	Group	Meaning
3	room	room number
42	agent	x coordinate
43	agent	y coordinate
52	agent	orientation (left/right)
27	beams	on/off
83	beams	beam countdown (on: 0, off: $36 \rightarrow 0$)
0	counter	counts from 0 to 255 and repeats
55	counter	death scene countdown
67	objects	Doors, skull, and key in 1st room
47	skull	x coordinate (1st and 2nd room)

5.3 A Case Study of Montezuma's Revenge

Montezuma's Revenge is widely known for its extremely sparse rewards and difficult exploration [1]. While our method does not outperform [1] on this game, we investigate the reasons behind this through various experiments. The experiment process below again demonstrates the importance of a hash function having the correct granularity and encoding relevant information for solving the MDP.

Our first attempt is to use game RAM states instead of image observations as inputs to the policy, which leads to a game score of 2500 with TRPO-BASS-SimHash. Our second attempt is to manually design a hash function that incorporates domain knowledge, called *SmartHash*, which uses an integer-valued vector consisting of the agent's (x, y) location, room number and other useful RAM information as the hash code. The best SmartHash agent is able to obtain a score of 3500. Still the performance is not optimal. We observe that a slight change in the agent's coordinates does not always result in a semantically distinct state, and thus the hash code may remain unchanged. Therefore we choose grid size s and replace the x coordinate by $\lfloor (x - x_{\min})/s \rfloor$ (similarly for y). The bonus coefficient is chosen as $\beta = 0.01\sqrt{s}$ to maintain the scale relative to the true reward[1] (see Table 7). Finally, the best agent is able to obtain 6600 total rewards after training for 1000 iterations ($1000\,\mathrm{M}$ time steps), with a grid size $s = 10$.

---

[1]The bonus scaling is chosen by assuming all states are visited uniformly and the average bonus reward should remain the same for any grid size.

Table 9: Performance comparison between state counting (left of the slash) and state-action counting (right of the slash) using TRPO-RAM-SimHash on Frostbite

	β						
k	0.01	0.05	0.1	0.2	0.4	0.8	1.6
64	879 / 976	2464 / 1491	2243 / 3954	2489 / 5523	1587 / 5985	1107 / 2052	441 / 742
128	1475 / 808	4248 / 4302	2801 / 4802	3239 / 7291	3621 / 4243	1543 / 1941	395 / 362
256	2583 / 1584	4497 / 5402	4437 / 5431	7849 / 4872	3516 / 3175	2260 / 1238	374 / 96

Table 8 lists the semantic interpretation of certain RAM entries in Montezuma's Revenge. SmartHash, as described in Section 5.3, makes use of RAM indices 3, 42, 43, 27, and 67. "Beam walls" are deadly barriers that occur periodically in some rooms.

During our pursuit, we had another interesting discovery that the ideal hash function should not simply cluster states by their visual similarity, but instead by their relevance to solving the MDP. We experimented with including enemy locations in the first two rooms into SmartHash ($s = 10$), and observed that average score dropped to 1672 (at iteration 1000). Though it is important for the agent to dodge enemies, the agent also erroneously "enjoys" watching enemy motions at distance (since new states are constantly observed) and "forgets" that his main objective is to enter other rooms. An alternative hash function keeps the same entry "enemy locations", but instead only puts randomly sampled values in it, which surprisingly achieves better performance (3112). However, by ignoring enemy locations altogether, the agent achieves a much higher score (5661) (see Figure 4). In retrospect, we examine the hash codes generated by BASS-SimHash and find that codes clearly distinguish between visually different states (including various enemy locations), but fails to emphasize that the agent needs to explore different rooms. Again this example showcases the importance of encoding relevant information in designing hash functions.

5.4 State and state-action counting

Continuing the results in Table 6, the performance of state-action counting is studied using the same experimental setup, summarized in Table 9. In particular, a bonus reward $r^+(s, a) = \frac{\beta}{\sqrt{n(s,a)}}$ instead of $r^+(s) = \frac{\beta}{\sqrt{n(s)}}$ is assigned. These results show that the relative performance of state counting compared to state-action counting depends highly on the selected hyperparameter settings. However, we notice that the best performance is achieved using state counting with $k = 256$ and $\beta = 0.2$.

References

[1] Bellemare, Marc G, Srinivasan, Sriram, Ostrovski, Georg, Schaul, Tom, Saxton, David, and Munos, Remi. Unifying count-based exploration and intrinsic motivation. In *Advances in Neural Information Processing Systems 29 (NIPS)*, pp. 1471–1479, 2016.

[2] Bloom, Burton H. Space/time trade-offs in hash coding with allowable errors. *Communications of the ACM*, 13(7):422–426, 1970.

[3] Cormode, Graham and Muthukrishnan, S. An improved data stream summary: the count-min sketch and its applications. *Journal of Algorithms*, 55(1):58–75, 2005.

[4] Duan, Yan, Chen, Xi, Houthooft, Rein, Schulman, John, and Abbeel, Pieter. Benchmarking deep reinforcement learning for continous control. In *Proceedings of the 33rd International Conference on Machine Learning (ICML)*, pp. 1329–1338, 2016.

[5] Fan, Li, Cao, Pei, Almeida, Jussara, and Broder, Andrei Z. Summary cache: A scalable wide-area web cache sharing protocol. *IEEE/ACM Transactions on Networking*, 8(3):281–293, 2000.

[6] Houthooft, Rein, Chen, Xi, Duan, Yan, Schulman, John, De Turck, Filip, and Abbeel, Pieter. VIME: Variational information maximizing exploration. In *Advances in Neural Information Processing Systems 29 (NIPS)*, pp. 1109–1117, 2016.

173   [7] Ioffe, Sergey and Szegedy, Christian. Batch normalization: Accelerating deep network training
174   by reducing internal covariate shift. In *Proceedings of the 32nd International Conference on*
175   *Machine Learning (ICML)*, pp. 448–456, 2015.

176   [8] Kingma, Diederik and Ba, Jimmy. Adam: A method for stochastic optimization. In *Proceedings*
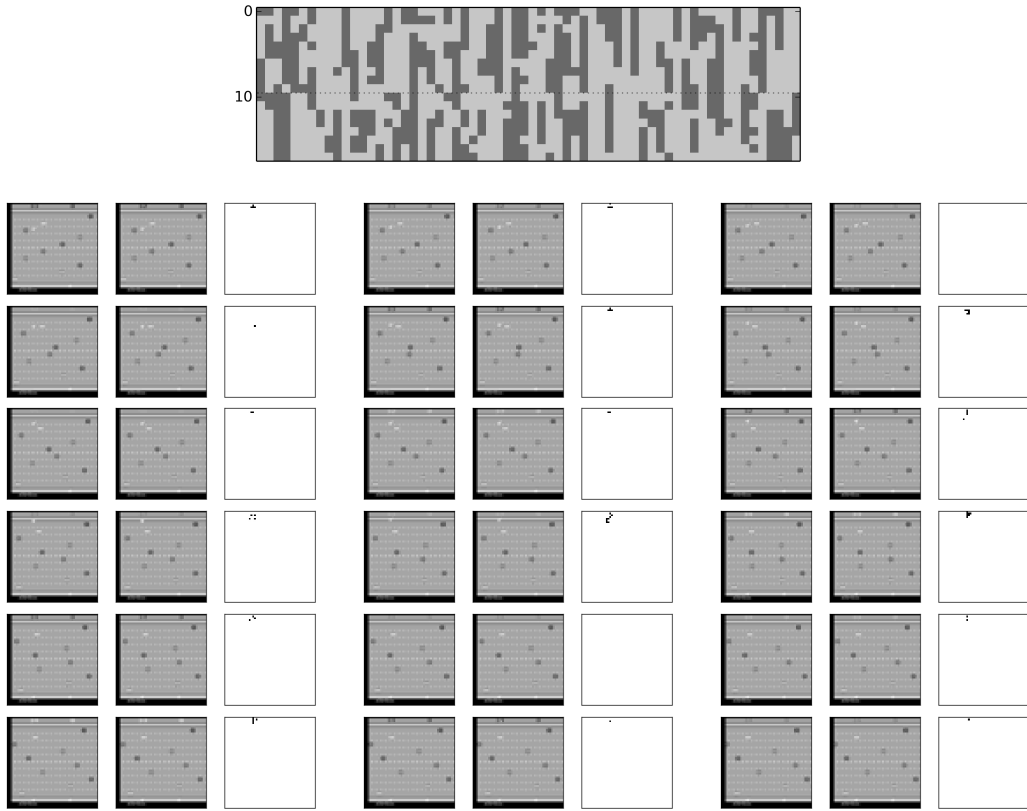177   *of the International Conference on Learning Representations (ICLR)*, 2015.

Figure 2: Freeway: subsequent frames and corresponding code (top); the frames are ordered from left (starting with frame number 0) to right, top to bottom; the vertical axis in the right images correspond to the frame number. Within each image, the left picture is the input frame, the middle picture the reconstruction, and the right picture, the reconstruction error.
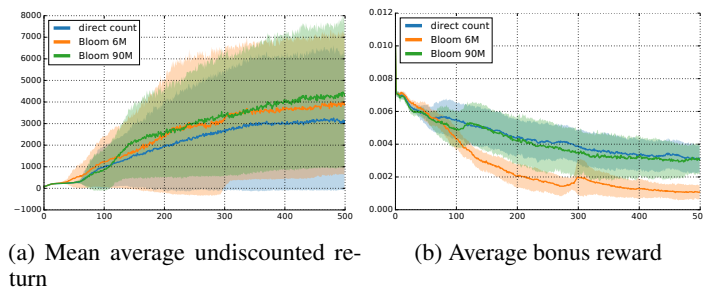

(a) Mean average undiscounted return

(b) Average bonus reward

Figure 3: Statistics of TRPO-pixel-SimHash ($k = 256$) on Frostbite. Solid lines are the mean, while the shaded areas represent the one standard deviation. Results are derived from 10 random seeds. Direct counting with a dictionary uses 2.7 times more computations than counting Bloom filters ($6\,\mathrm{M}$ or $90\,\mathrm{M}$).
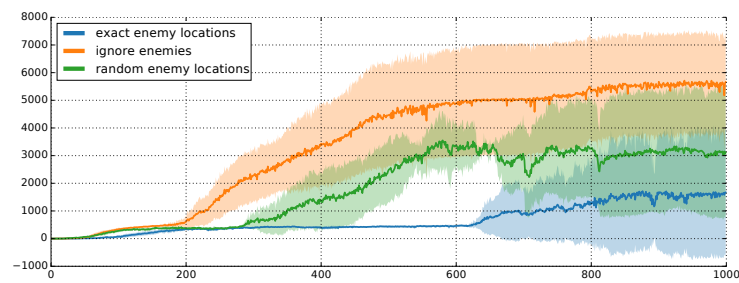
9

Figure 4: SmartHash results on Montezuma's Revenge (RAM observations): the solid line is the mean average undiscounted return per iteration, while the shaded areas represent the one standard deviation, over 5 seeds.